2018

Electrical-Power Constrained Attitude Steering

Marsh, Harleigh C.; Karpenko, Mark; Gong, Qi

American Astronomical Society

Marsh, H. C., Karpenko, M., and Gong, Q., "Electrical-Power Constrained Attitude Steering", AAS/AIAA Astrodynamics Specialist Conference, August 20-24, 2017, Stevenson, WA. Paper number: AAS 17-774.
http://hdl.handle.net/10945/65808

ASTRODYNAMICS 2017

Volume 162
Part I
ADVANCES IN THE ASTRONAUTICAL SCIENCES

Edited by
Jeffrey S. Parker
John H. Seago
Nathan J. Strange
Daniel J. Scheeres

Proceedings of the AAS/AIAA Astrodynamics Specialist Conference held August 20–24, 2017, Columbia River Gorge, Stevenson, Washington, U.S.A.

Published for the American Astronautical Society by
Univelt, Incorporated, P.O. Box 28130, San Diego, California 92198
Web Site: http://www.univelt.com

AAS Publications Office
P.O. Box 28130
San Diego, California 92198

Affiliated with the American Association for the Advancement of Science
Member of the International Astronautical Federation

First Printing 2018

Library of Congress Card No. 57-43769

ISSN 0065-3438

ISBN 978-0-87703-645-6 (Hard Cover Plus CD ROM)
ISBN 978-0-87703-646-3 (Digital Version)

Published for the American Astronautical Society
by Univelt, Incorporated, P.O. Box 28130, San Diego, California 92198
Web Site: http://www.univelt.com

Printed and Bound in the U.S.A.

ELECTRICAL-POWER CONSTRAINED ATTITUDE STEERING

Harleigh C. Marsh,* Mark Karpenko† and Qi Gong‡

This paper examines the effectiveness of reducing the energy consumption of a reaction-wheel array over the course of a slewing maneuver by steering the attitude of the spacecraft, in situations where it is not possible to command the reaction wheel torque directly. To explore this avenue, a set of constrained nonlinear non-smooth L1 optimal-control problems are formulated and solved. It is demonstrated that energy consumption, dissipative losses, and peak-power load, of the reaction-wheel array can each be reduced substantially, by controlling the input to the attitude control system through attitude steering, thereby avoiding software modifications to flight software.

INTRODUCTION

Power is *the* driving resource upon a spacecraft and impacts every facet and phase of its existence, whether from the initial design phase, where resources are allocated for energy storage that effect the payload of the spacecraft, or whether till late mission life when power systems begin to degrade. Power directly effects the efficacy of scientific data collection, from running the instruments, to operating the attitude control system (ACS) which slews the spacecraft to orientations of interest. Minimizing power and energy demands has the potential of prolonging the operational lifespan of the spacecraft, thereby enhancing the scientific utility of the spacecraft, and lowering the overall monetary-cost of a mission. Prolonging life expectancy is especially pertinent given the recent failures of the reaction wheel actuators on the NASA's Kepler, Mars Odyssey, and Dawn spacecrafts [1], and the anomalies detected on NASA's Cassini spacecraft [2] during it's more than nineteen year exploration. Power not only has an effect on the efficacy of science, but has a fundamentally direct and meaningful impact from an econometric standpoint, as well as from a social-media standpoint when considering the public's response to scientific failures.

Synthesizing the above exposition, it is apparent that minimizing the power or energy required to perform a slew is a highly desirable goal. Situations in which the power management becomes highly beneficial, is late in mission life when power systems begin to degrade. Due to the high cost and invested effort involved with a spacecraft, it behooves the science community to attempt to keep scientific data collections active as long

* PhD Candidate and corresponding author., Department of Applied Mathematics and Statistics, University of California Santa Cruz, Santa Cruz, California, 95064, USA. E-mail: hcmarsh@soe.ucsc.edu.
† Research Associate Professor, Department of Mechanical and Aerospace Engineering, Naval Postgraduate School, Monterey, CA 93943, USA, E-mail: mkarpenk@nps.edu.
‡ Associate Professor., Department of Applied Mathematics and Statistics, University of California Santa Cruz, Santa Cruz, California, 95064, USA. E-mail: qigong@soe.ucsc.edu.

as possible, extending the operation of the spacecraft well-past the original mission requirements. An example exemplifying longevity past original mission requirements, was NASA's Far Ultraviolet Spectroscopic Explorer (FUSE) spacecraft, whose three year mission was extended to over eight years of scientific observations and collections [3]. Deep-space operations are another facet exemplifying the necessity to preserve power: Solar cells are a renewable source of energy, but are only effective up to the orbit of Mars; beyond that distance the solar radiant flux is not adequate to power spacecraft, and therefore alternate methods to generate power, such as thermoelectric heat engines are required to generate energy for deep-space missions [4]. Because the power output of radioisotope thermoelectric generators which drive deep-space spacecraft fade over time, NASA has a vested interest in both extracting more power, along with increasing the amount of time before the power-output profiles degrade [5]. Regardless of the power and energy source, as a spacecraft ages onboard power generation and energy storage systems capabilities begin to degrade. Consider Voyager 1, which has had to have its scientific instruments shut off one by one, as a result *not* of malfunction, but rather as a result of dwindling power-output profiles [6]. One approach to possibly ameliorate the requirement for more power, especially when power systems begin to degrade, is to reduce the power requirements of the attitude control system. Reaction wheels can be a considerable load upon a spacecraft [7]. The execution of slew maneuvers, notably large-angle slews, may cause short-in-duration though large-in-magnitude power demands, which in turn may cause electrical transients [8]. These transients can degrade power quality across the entire electrical bus, which often services sensitive scientific instruments as well as the attitude control system. They can also potentially create a violation of power constraints placed upon the spacecraft. Similarly, in a system with degraded power margins, peak power loads (which can occur during the execution of a large angle slew) can generate electrical surges [8]. Reducing power demands can potentially bring greater utility out of a spacecraft, especially late in operational life well past its original mission.

While minimizing the cumulative electric power consumed by the reaction wheel array is highly favorable, solving the problem poses significantly challenging from both a computational as well theoretical standpoint. These challenges arise due to the fact that the electric power-input equation is nonsmooth [9], and it is this challenge which has lead many researchers to instead minimize *proxies* to the reaction wheel power equation, such as mechanical power. It was shown in both [8], that minimizing the electric power-input equation may be formulated as a L^1 optimal control problem. An approach to minimize the power-input equation was devised in [8] by generating an equivalent *smooth* formulation, by virtue of lifting the dimensionality of the original nonsmooth problem via the addition of ancillary decision variables, and appropriate constraints upon these variables. In a setting where the reaction wheel motor torques may not be directly controlled and that modifications to the flight software are unfeasible, e.g. due to cost, minimum energy solutions must be able to work with a heritage attitude control system. One approach to reduce the energy requirements of such systems is by steering the attitude of the spacecraft based on the knowledge of the underlying control allocation scheme (e.g. least-squares), spacecraft parameters (e.g. inertia tensor), and relevant constraints (e.g. saturation limits). This allows the behavior of the attitude control system to be modified without the need to otherwise alter the flight control logic.

A family of electrical power and energy metrics were derived in [9], to study the relationship between electrical energy and transfer time between on-and off-eigenaxis maneuvering. This study was from the perspective of a global approach within the framework of optimal control, with a performance index which minimized dissipative losses of the reaction wheels, and under the assumption that the reaction wheels can be directly controlled. An early work in optimal energy slews was seen in [10], where the copper loss of a single reaction wheel motor was minimized. References of [10–12] also approached energy minimization of reaction wheel spacecraft through an optimal control framework. Although each approach to minimize energy varied in either performance index or number of reaction wheels, they matched in control input, with each assuming that the reaction wheel motor torques may be *directly controlled*. A feedback solution to the minimization of the instantaneous L^2 norm of mechanical power to a redundant actuator array was devised in [13]. This was accomplished by augmenting the instantaneous reaction wheel torque profiles from a least-squares control allocation through the addition of null motions. The efficacy of null motions to reduce the energy associated to a least-squares control allocation scheme was further investigated in [14], although under a performance index that assumed power may be regenerated when a reaction wheel decelerates. A feedback control law for simultaneous attitude and power tracking was developed in [15], where null motions were

utilized to track a power profile. The problem of distributing the control torque unto the reaction wheels, to minimize the instantaneous L^1 norm of mechanical power, was posed as a constrained convex optimization problem in [16], and solved through an application of lexicographic optimization.

A point of commonality among the literature which seek slewing strategies for the reduction of energy, is the assumption that reaction wheel inputs may be *directly* accessed and modified. Schemes which seek to reduce energy consumption either take control to be the motor torques generated by the reaction wheels, or *directly* augment the torque allocation scheme e.g. through the application of null motions. This assumption is tantamount to assuming that the attitude control system is equipped with an accessible feed-forward component, which may not be the case. Indeed, in a conventional ACS it is typical that attitude is taken as input.[17] Therefore in the quest for energy-reducing schemes, there exist situations in which the control allocation performed by the spacecraft needs to be incorporated when designing a solution. That there exists a situation in which the reaction wheel motor torques can not be *directly* modified nor accessed raises, then the question of how minimum energy slews can be implemented when the *spacecraft* is in control of the torque allocation. The objective of this paper is to seek minimum energy slews for the case when the reaction wheels can not be directly controlled. The approach taken by this paper is to steer the attitude of the spacecraft, which may be thought of as determining a path for the boresight, with the goal of obtaining a minimum electric energy maneuver. Therefore, the goal of this work is to develop minimum energy maneuvers, by steering the attitude of the spacecraft, under the knowledge of the control allocation scheme implemented by the spacecraft. The control allocation scheme, is assumed to be L^2 allocation, i.e: least-squares allocation. In order to obtain minimum energy attitude steering, a fixed-endpoint, fixed-time optimal control problem is formulated in this paper, denoted problem A_s. The formulation directly considers the nonlinear rotational dynamics, which are required for the analysis of large angle slews. Also considered in the formulation are practical constraints upon both the state and the control variables, which arise in an operational setting. For example hardware constraints involving the saturation limits of the rate gyros, and the maximum speed and torque authority of the reaction wheels. Lastly, the formulation *directly* considers the nonsmooth reaction wheel power-input equation. This nonsmooth, nonlinear optimal control problem is numerically solved using Pseudospectral (PS) optimal control theory [18–23] implemented in the software-package DIDO. An attractive feature of the pseudospectral optimal control theory framework, is the ability to generate adjoint variables from the numerical solutions via the Covector Mapping Theorem [24–26]. This enables the verification of the optimality of numerical solutions to problem A_s against the necessary conditions for optimality given by application of Pontryagin's Minimum Principle. Another reason for choosing the PS framework, is that solutions derived from PS optimal control methods have been proven to be successfully implemented in flight, from achieving successful ground tests [27], to the landmark achievements of both the Zero & Optimal Propellant Maneuvers of the International Space Station [28–31], and to the first flight-implementation of a shortest-time slewing maneuver [32–34].

The remainder of this paper is organized as follows: First the rotational dynamics of a spacecraft employing a L^2 allocation scheme is derived. Following the dynamics, the reaction wheel power model and energy metrics are presented. The next section presents a set of high dimensional nonlinear optimal control problem formulations for the minimization of electrical energy by steering the attitude of the spacecraft, along with the necessary conditions derived from Pontryagin's Minimum Principle. The last section demonstrates the efficacy of steering the attitude of the spacecraft by comparing the feedback implementation of the designed minimum electric energy attitude steering maneuver against a conventional eigenaxis maneuver.

ATTITUDE DYNAMICS WITH LEAST-SQUARES ALLOCATION

The rotational dynamics for a spacecraft which implements a least-squares control allocation scheme for attitude control may be derived from first principals by considering the conservation of angular momentum in the inertial frame $\mathcal{N}$:

$$H^{\mathcal{N}}(t) = \int_0^t \tau_{\text{ext}}^{\mathcal{N}}(s)\, ds + H^{\mathcal{N}}(0),$$

where $H^{\mathcal{N}}(t) \in \mathbb{R}^3$ is the total angular momentum, at time t, of the spacecraft expressed in the inertial frame, and $\tau_{\text{ext}}^{\mathcal{N}}(t)$ is the vector representing the total external torque (e.g.: solar, atmospheric, magnetic) acting upon

the spacecraft. By the application of the transport theorem [35]

$$\tau_{\text{ext}}^{\mathcal{N}}(t) = \frac{\mathrm{d}}{\mathrm{d}t} H^{\mathcal{N}}(t) = \frac{\mathrm{d}}{\mathrm{d}t} H^{\mathcal{B}}(t) + \omega(t) \times H^{\mathcal{B}}(t), \tag{1}$$

where $H^{\mathcal{B}}(t), \omega(t) \in \mathbb{R}^3$ are time varying vectors of the angular momentum and angular velocity of the spacecraft represented in the body frame $\mathcal{B}$. The total angular momentum of the spacecraft in the body frame may be decomposed into contributions from the spacecraft body as well as from the reaction wheels :

$$H^{\mathcal{B}}(t) \triangleq H_{\text{sc}}^{\mathcal{B}}(t) + H_{\text{rw}}^{\mathcal{B}}(t) = J_{\text{sc}}\omega(t) + Ah(t),$$

where $J_{\text{sc}} \in \mathbb{R}^{3\times 3}$ is the spacecraft inertia tensor, $A \triangleq \left[a_1 | \ldots | a_{N_{\text{rw}}}\right] \in \mathbb{R}^{3\times N_{\text{rw}}}$ is the matrix which projects from the reaction wheel frame, onto the spacecraft body frame. Each a_i gives the orientation of the ith reaction-wheel spin axes in relation to the spacecraft body frame. Both J_{sc} and A are assumed to be time invariant with respect to the spacecraft body frame. The vector $h(t) \in \mathbb{R}^{N_{\text{rw}}}$ is comprised of the angular momenta of each reaction wheel in relation to its spin axis. The rate of change of the spacecraft with respect to the body frame is given as

$$\frac{\mathrm{d}}{\mathrm{d}t} H^{\mathcal{B}}(t) = \frac{\mathrm{d}}{\mathrm{d}t}(J_{\text{sc}}\omega(t) + Ah(t)) = J_{\text{sc}}\dot{\omega}(t) + A\dot{h}(t),$$

under the assumption that J_{sc} and A are time invariant, and noting that the relative motion between the reaction wheel actuator frame and the spacecraft body is null. Therefore Eq. (1) may be expanded as

$$\tau_{\text{env}}(t) + \tau_{\text{mms}}(t) = J_{\text{sc}}\dot{\omega}(t) + A\dot{h}(t) + \omega(t) \times (J_{\text{sc}}\omega(t) + Ah(t)), \tag{2}$$

where the external torque acting upon the spacecraft, $\tau_{\text{ext}}^{\mathcal{N}}(t)$, has been decomposed into environmental torques, as well as torque from the spacecraft momentum management system (MMS). A reasonable assumption upon the rotational dynamics model, is that total external torques in Eq. (2) may be taken as null during the course of a slewing maneuver. This assumption is quantified as reasonable because the MMS is only used for momentum dumping and is generally not active during a slew. Moreover, the magnitude of the environmental torques acting upon the spacecraft are typically quite small during the course of a slewing maneuver.

Turning attention to the reaction wheel dynamics, the angular momentum of each reaction wheel is modeled by the following equation:

$$h(t) = J_{\text{rw}}\Omega_{\text{rw}}(t) - J_{\text{rw}}A^{\intercal}\omega(t), \tag{3}$$

where J_{rw} is a diagonal matrix with N_{rw} entries along the main-diagonal, whose i-th entry is the inertia of the i-th reaction wheel, which is assumed to be time invariant with respect to the spacecraft body frame. The vector $\Omega_{\text{rw}}(t) \in \mathbb{R}^{N_{\text{rw}}}$ is comprised of the angular rates of the reaction wheels about their respective spin axes. The angular momentum increment resulting from the spacecraft relative to the wheels is described by $J_{\text{rw}}A^{\intercal}\omega(t)$. Because reaction wheels are normally operated at a bias rate, $\Omega_{\text{rw},i}(t) \gg a_i^{\intercal}\omega(t)$ so Eq. (3) may be reasonably approximated as

$$h(t) = J_{\text{rw}}\Omega_{\text{rw}}(t). \tag{4}$$

Noting that in Eq. (4) the reaction wheel control torque is given as $\tau_{\text{rw}}(t) = \dot{h}(t)$, the torque upon the spacecraft in the body frame is expressed by

$$\tau_{\text{sc}}^{\mathcal{B}}(t) = \dot{H}_{\text{rw}}^{\mathcal{B}}(t) = A(-\dot{h}(t)) = -A\tau_{\text{rw}}(t).$$

Therefore, under a least-squares control allocation scheme, the standard selection of reaction wheel motor torques to produce a commanded body torque, is taken as

$$\tau_{\text{rw}}(t) = -A^{+}\tau_{\text{sc}}^{\mathcal{B}}(t),$$

where A^{+} is the standard Moore-Penrose inverse of the matrix A, that gives the least-squares solution in terms of commanded torques [17]. Synthesizing the above derivations, the equations of rotational motion of

a spacecraft which implements a standard Moore Penrose control allocation scheme with N_{rw} reaction wheels is given as

$$\begin{bmatrix} \dot{\omega}(t) \\ \dot{\Omega}_{\text{rw}}(t) \end{bmatrix} = \begin{bmatrix} J_{\text{sc}}^{-1}(AA^{+}\tau_{\text{sc}}^{\mathcal{B}}(t) - \omega(t) \times (J_{\text{sc}}\omega(t) + AJ_{\text{rw}}\Omega_{\text{rw}}(t))) \\ -J_{\text{rw}}^{-1}A^{+}\tau_{\text{sc}}^{\mathcal{B}}(t) \end{bmatrix}$$

Lastly, the attitude kinematics are considered to complete the spacecraft model. The attitude of the spacecraft is modeled using a quaternion parameterization. The choice of quaternions is by virtue of being free of singularities or discontinuities inherit to three-parameter representations [36]. The quaternion parameterization given by

$$q = \left[e_1 \sin\left(\tfrac{\Phi}{2}\right), \quad e_2 \sin\left(\tfrac{\Phi}{2}\right), \quad e_3 \sin\left(\tfrac{\Phi}{2}\right), \quad \cos\left(\tfrac{\Phi}{2}\right)\right]^{\mathsf{T}} \in \mathbb{R}^4,$$

where $e = [e_1, e_2, e_3]^{\mathsf{T}}$ is the eigenaxis and Φ is the rotation angle about the eigenaxis. The quaternion kinematic differential equations are described by the following system [17]:

$$\dot{q} = \frac{1}{2}\mathcal{Q}(\omega)q, \tag{5}$$

where $\mathcal{Q}(\omega)$ is a skew-symmetric matrix given as

$$\mathcal{Q}(\omega) \triangleq \begin{bmatrix} 0 & \omega_3 & -\omega_2 & \omega_1 \\ -\omega_3 & 0 & \omega_1 & \omega_2 \\ \omega_2 & -\omega_1 & 0 & \omega_3 \\ -\omega_1 & -\omega_2 & -\omega_3 & 0 \end{bmatrix}.$$

REACTION WHEEL POWER MODEL & ENERGY METRICS

From the standpoint of minimizing the energy consumption of the reaction wheels to perform a slew, the electric motors which drive the reaction wheels are modeled as direct current (DC) motors in steady state [37]. By this model choice, inductive losses are assumed to be small compared to the DC power loss in the windings. In steady state, the load torque of a single motor is the sum of the commanded-torque, τ_{rw} and a drag term, τ_{drag}, associated to the wheel speed. For this model, the angular velocity of the motor shaft is taken as the speed of the reaction wheel Ω. Identifying that the load torque must be balanced against the average current flowing through the motor windings I, gives the following equation:

$$I(t) = \frac{1}{K_\tau}(\tau_{\text{rw}}(t) + \tau_{\text{drag}}(t)), \tag{6}$$

where K_τ is the motor torque constant. The reaction wheel drag torque (i.e. friction) is modeled linearly, with a viscous friction term $\tau_{\text{drag}}(t) = \beta_{\text{v}}\Omega(t)$, where β_{v} correspond to the coefficient for viscous friction. The equation which describes the supply voltage to the DC motor in steady state is given as

$$V_{\text{s}}(t) = I(t)R + K_{\text{V}}\Omega(t), \tag{7}$$

where V_{s} is the supply voltage, R is the armature resistance, and K_{V} is the back electromotive force (EMF) constant. Note that, for SI units, $K_\tau = K_{\text{V}}$. Expanding the electrical power-input equation, $\mathcal{P}(t) = I(t)V_{\text{s}}(t)$, using Eqs. (6) and (7), three main groups appear: Two which represent instantaneous dissipative losses occurring in the DC motor, and one as a mechanical power term:

$$\mathcal{P}(t) = \underbrace{\frac{R}{K_{\text{T}}^2}(\tau_{\text{rw}}(t) + \beta_{\text{v}}\Omega(t))^2}_{\text{Copper Loss}} + \underbrace{\tau_{\text{rw}}(t)\Omega(t)}_{\text{Mechanical Power}} + \underbrace{\beta_{\text{v}}\Omega^2(t)}_{\text{Friction Loss}}. \tag{8}$$

The copper-loss term represents power lost as heat in the windings, and is proportional to the amount of torque effort requested. The friction-loss term represents the loss incurred to overcome wheel drag, and is proportional to the magnitude of the angular velocity of the reaction wheel.

During a slew, the motor which drives a reaction wheel may alternate between acting as a source ($\mathcal{P}(t) > 0$) or acting as a load ($\mathcal{P}(t) \leq 0$). For a system implementing a regenerative scheme, energy can be restored to the system while a motor acts as a source. In practice though, regenerative methods are typically not implemented for a spacecraft, so generated power is shunted to ground via a ballast resistor [37]. Because bus power is only being utilized by the reaction wheels when $\mathcal{P} > 0$, the total electric power-input to an array of N_{rw} reaction wheels at any instant in time is given by:

$$\mathcal{P}_{\text{array}}(t) \triangleq \sum_{i=1}^{N_{\text{rw}}} \{\mathcal{P}_i(t)\}^+ . \tag{9}$$

Equation (9) measures the power-input of the reaction wheel array. The operator $\{\cdot\}^+$ is defined as

$$\{f(t)\}^+ = \begin{cases} f(t) & \text{if } f(t) > 0 \\ 0 & \text{if } f(t) \leq 0 \end{cases} \tag{10}$$

The total energy required by the reaction wheel array to perform a slew over a transfer time $[0, T]$ is obtained by integrating Eq. (9):

$$\mathcal{E} \triangleq \int_0^T \mathcal{P}_{\text{array}}(t)\, dt. \tag{11}$$

From Eqs. (9) & (10), it is clear that the reaction wheel power equation is a nonsmooth function. Therefore by taking the cost functional to an optimal control problem as $\mathcal{E}$ in Eq. (11), in an effort to minimize the energy required to perform a slew, results with a nonsmooth formulation with respect to *both* state and control. Because the non-differentiability of the cost functional is with respect to control as well as state, using Eq. (11) poses both significant numerical as well as theoretical challenges. The manner in which these challenges are overcome are addressed in the next section.

Along with Eq. (9), which describes the total amount of energy consumed by the reaction wheel array, another useful energy metric is the cumulative amount of dissipated energy by the reaction wheel array. The metric measuring the total dissipation loss incurred throughout the course of the slewing maneuver is defined as the total amount of copper and frictional losses incurred by the motors over the course of a slewing maneuver:

$$\mathcal{E}_{total}^{loss} \triangleq \sum_{i=1}^{N_{\text{rw}}} \mathcal{C}_{\text{loss},i} + \sum_{i=1}^{N_{\text{rw}}} \mathcal{F}_{\text{loss},i},$$

where, for each $i = 1, \ldots, N_{\text{rw}}$,

$$\mathcal{C}_{\text{loss},i} \triangleq \int_0^T I_i^2(t) R\, dt, \text{ and } \mathcal{F}_{\text{loss},i} \triangleq \int_0^T \beta_{\text{v}} \Omega_{\text{rw},i}^2(t)\, dt.$$

MINIMUM ENERGY ATTITUDE STEERING

In this section, the dynamical model for a spacecraft implementing a least-squares control allocation scheme, and the energy model for reaction wheel actuators, are incorporated into an optimal control formulation for the minimizing the electrical energy required to perform a slew. The slewing maneuvers of interest to this work, are rest-to-rest maneuvers from an initial orientation given by $q^0 \triangleq \left[e_0 \sin\left(\frac{\Phi_0}{2}\right), \cos\left(\frac{\Phi_0}{2}\right)\right]^{\mathsf{T}} \in \mathbb{R}^4$ to a final orientation given by $q^f \triangleq \left[e_f \sin\left(\frac{\Phi_f}{2}\right), \cos\left(\frac{\Phi_f}{2}\right)\right]^{\mathsf{T}} \in \mathbb{R}^4$, with $\omega^0 = \omega^f = 0 \in \mathbb{R}^3$. Other scenarios can be evaluated by appropriately altering the boundary conditions.

The optimal control formulation presented in this section incorporates practical constraints upon both state and control, each in-line with a typical operational scenario: (*i*) Reaction wheel speed-bias, $\Omega_{\text{bias}} \in \mathbb{R}$, is enforced per wheel to avoid operating the wheels near zero-speed. (*ii*) Per axis limits, $\omega_{\text{max}} \in \mathbb{R}$, are imposed upon the spacecraft angular rate to avoid rate gyro saturation. (*iii*) Per wheel momentum storage, $\Omega_{\text{max}} \in \mathbb{R}$,

and torque authority, $\tau_{\max} \in \mathbb{R}$, constraints are also considered. The optimal control problem formulation is presented as follows, and is denoted hereafter as problem "A_{ns}":

$$
(A_{\text{ns}}) \left\{ \begin{array}{ll}
\text{State:} & x = [q, \omega, \Omega_{\text{rw}}]^{\mathsf{T}} \in \mathbb{R}^{7+N_{\text{rw}}}, \ \text{Control:} \ u = \tau_{\text{sc}}^{\mathcal{B}} \in \mathbb{R}^3, \\
\text{Minimize:} & J\left[x(\cdot), u(\cdot)\right] = \displaystyle\int_0^T \sum_{i=1}^{N_{\text{rw}}} \{\mathcal{P}_i\}^+ \, dt \\
\text{Subject To:} & \\
& \begin{bmatrix} \dot{q} \\ \dot{\omega} \\ \dot{\Omega}_{rw} \end{bmatrix} = \begin{bmatrix} \frac{1}{2}\mathcal{Q}(\omega) q \\ J_{\text{sc}}^{-1}(AA^{+}\tau_{\text{sc}}^{\mathcal{B}} - \omega \times (J_{\text{sc}}\omega + AJ_{\text{rw}}\Omega_{\text{rw}})) \\ -J_{\text{rw}}^{-1}A^{+}\tau_{\text{sc}}^{\mathcal{B}} \end{bmatrix} \\
& x(0) = \left[q^0, \ \omega^0, \ \Omega_{\text{bias}}\right]^{\mathsf{T}} \in \mathbb{R}^{7+N_{\text{rw}}} \\
& x(t_f) = \left[q^f, \ \omega^f, \ \Omega_{\text{bias}}\right]^{\mathsf{T}} \in \mathbb{R}^{7+N_{\text{rw}}} \\
& |\omega_i| \leq \omega_{\max}, \ \forall\, i = 1, 2, 3 \\
& |\Omega_{\text{rw},i}| \leq \Omega_{\max}, \ \forall\, i = 1, \ldots, N_{\text{rw}} \\
& \left|(A^{+}\tau_{\text{sc}}^{\mathcal{B}}(t))_i\right| \leq \tau_{\max}, \ \forall\, i = 1, \ldots, N_{\text{rw}}
\end{array} \right. \tag{12}
$$

The state of the system consists of the attitude of the spacecraft in quaternion parameterization, the angular velocity of the spacecraft body (with respect to the body frame), and the reaction wheel angular velocities (about their individual spin axes). Because the spacecraft is assumed to be allocating control authority to the reaction wheels (through a least-squares allocation scheme) the control vector is taken as the three-vector of torques acting on the spacecraft body. The cost functional is taken with the reaction wheel power-input of the reaction wheel array as the running cost; therefore problem A_{ns} minimizes the energy required to perform a slew. The upper bound on the transfer time for the slew is given by T. For a minimum-energy problem, it is typical for the final time to extend to the right of the allowed horizon, i.e. $t_f > T$. Therefore, for the problem to be feasible, the value of T must be, at minimum, the transfer-time of the shortest-time maneuver, t_{STM}, for the same parameters and boundary conditions. From this point of view, a minimum energy shortest-time maneuver can be determined by setting $T = t_{\text{STM}}$. The transfer time of the a shortest time maneuver, t_{STM}, can be determined by a simple modification to the cost functional by rewriting $J\left[x(\cdot), \tau_{\text{rw}}(\cdot), t_f\right] = t_f$ and allowing $0 \leq t \leq \infty$. The boundary conditions and the dynamics comprise the rest-to-rest attitude maneuvers and dictate the evolution of the system. Last in the formulation are the constraints associated to rate-gyro saturation, maximum reaction wheel speed, and torque generatable by the reaction wheels. Given that the control is taken as the spacecraft body torques and not the reaction wheel motor torques themselves, which have a hard-limit on maximum generatable torque, $\tau_{\max}$, an additional path constraint is required. To accommodate the hardware limits of maximum torque generatable by the reaction wheels, $\tau_{\max}$, requires the incorporation of N_{rw} paths constraints into the formulation, given by $\left|(A^{+}\tau_{\text{sc}}^{\mathcal{B}}(t))_i\right| \leq \tau_{\max}, \ \forall\, i = 1, \ldots, N_{\text{rw}}$.

Problem A_{ns} does not enforce any constraints to constrain the attitude maneuver to be an eigenaxis slew. Therefore, off-eigenaxis slewing maneuvers are feasible to problem A_{ns}, and hence are potential solutions to problem A_{ns} should they be more advantageous with respect to the energy metric when meeting a given constraint on the slew time. Given the extra degrees of freedom that off-eigenaxis maneuvering permits, coupled with the non-symmetric inertia tensors of real-world spacecraft, it seems plausible that off-eigenaxis maneuvers would be more advantageous with respect to energy when compared to their eigenaxis counterparts. Indeed this is the case as seen in [9]. The analysis to follow in this paper is concerned with evaluating the energy requirements under attitude steering, for off-eigenaxis slew profiles against the conventional eigenaxis control logic [17]. To achieve an eigenaxis maneuver under a slew-rate constraint, the A_{ns} formulation presented in Eq. (12) requires two alterations: (*i*) To constrain the motion of the spacecraft, the angular velocity vector of the spacecraft must always be collinear with the eigenaxis [38]. Including the following path-constraint as part of problem A_{s} achieves this goal:

$$
\omega(t) \times e(q^0, q^f) = 0 \in \mathbb{R}^3, \ \forall t, \tag{13}
$$

It is noted in Eq. (13), that the eigenaxis e is a function of the initial and final attitude quaternion. For an eigenaxis slew it is also necessary to enforce a spherical slew rate constraint in concerns of saturating the rate

gyros. This can be done by including an additional path constraint of the form $\|w\|_2 \leq \omega_{\max}$, which replaces the three path constraints $|\omega_i| \leq \omega_{\max},\ \forall i = 1, 2, 3$.

Managing the Nonsmooth Energy Formulation

Problem A_{ns}, due to the choice of cost functional is nonsmooth with respect to both state and control. This formulation is particularly challenging, posing both numerical as well as theoretical challenges because the cost functional is not differentiable with respect to neither state nor control. For instance, the non-differentiability with respect to state precludes the direct application Pontryagin's minimum principal to problem A_{ns}. The intricate and exotic framework of nonsmooth analysis [39, 40] is required in order to apply PMP to problem A_{ns}. Therefore, the identification and analysis of the necessary conditions to problem A_{ns} as a means to validate optimality to an obtained solution, is a nontrivial task. It is because of these challenges, that it is common to minimize *proxies* to Eq. (11), rather than Eq. (11) directly. In this work, the electric energy model in Eq. (11) is directly minimized. The manner in which the difficulties outlined earlier are overcome, is by recasting problem A_{ns} into an equivalent *smooth* formulation. A smooth formulation of problem A_{ns} may be obtained by lifting the dimensionality of the formulation through the addition of ancillary decision variables, along with appropriate constraints on the decision variables, as was done in [8]. In this section, the approach from [8] is briefly discussed and then applied to problem A_{ns}.

A reaction wheel only draws power when the electric motor which drives the wheel, the acts as a load. This behavior corresponds to when Eq.(8) is positive. The positive-only portion of the reaction wheel power-input equation in Eq.(9) may be cast as

$$\{\mathcal{P}_i(t)\}^+ = \frac{1}{2}(\mathcal{P}_i(t) + |\mathcal{P}_i(t)|) \quad \text{for each } i = 1, \ldots, N_{\text{rw}}. \tag{14}$$

Due to the presence of the absolute value sign in Eq. (14), problem A_{ns} is recognized as a nonlinear L^1 optimal control problem. Under the relation in Eq. (14) the running cost functional may now be separated into smooth and nonsmooth portions:

$$\text{Minimize:} \quad J\left[x(\cdot), u(\cdot)\right] = \frac{1}{2}\int_0^T \left\{\sum_{i=1}^{N_{\text{rw}}} \mathcal{P}_i(t) + \sum_{i=1}^{N_{\text{rw}}} |\mathcal{P}_i(t)|\right\} dt$$

Based on this reformulation of the cost functional in problem A_{ns}, its is clear that the only terms involving the absolute value operator must transformed to obtain an equivalent smooth formulation. An appropriate choice of ancillary decision variables is based off of [19, 41], for each $i = 1, \ldots, N_{\text{rw}}$: $z_i(t) \triangleq \mathcal{P}_i(t)$. Next, the positive and negative portions of z are defined as

$$z_{a,i}(t) \triangleq \{\mathcal{P}_i(t)\}^+ \qquad \text{and} \qquad z_{b,i}(t) \triangleq \{-\mathcal{P}_i(t)\}^+, \tag{15}$$

where $\{\cdot\}^+$ is defined in Eq. (10). By the manner in which z, z_a, and z_b are defined, the following relationships hold for all $t \in [t_0, t_f]$ [8]:

$$z_i(t) = z_{a,i}(t) - z_{b,i}(t), \qquad |z(t)| = z_a(t) + z_b(t), \qquad z_a(t), z_b(t) \geq 0. \tag{16}$$

Because the cost functional is minimizing the absolute value of z, each ancillary control variable as defined in Eq. (15) are obtained through the path constraints of Eq. (16) along with the path constraints:

$$z_{a,i} - \mathcal{P}_i \geq 0,\ \forall i = 1, \ldots, N_{\text{rw}} \qquad \text{and} \qquad z_{b,i} + \mathcal{P}_i \geq 0,\ \forall i = 1, \ldots, N_{\text{rw}}, \tag{17}$$

Amalgamating Eqs. (16) and (17), an equivalent smooth formulation to problem A_{ns} may be arrived upon,

and is given in the following formulation(which, hereafter is referred to as problem A_s):

$$
(A_s)\begin{cases}
\text{State:} & x = [q, \omega, \Omega_{rw}]^{\mathsf{T}} \in \mathbb{R}^{7+N_{\text{rw}}} \\
\text{Control:} & u = \left[\tau_{\text{sc}}^{\mathcal{B}},\ z_{a,1},\ z_{b,1},\ \ldots,\ z_{a,N_{\text{rw}}},\ z_{b,N_{\text{rw}}}\right]^{\mathsf{T}} \in \mathbb{R}^{3+2N_{\text{rw}}} \\
\text{Minimize:} & J\left[x(\cdot), u(\cdot)\right] = \dfrac{1}{2}\displaystyle\int_0^T \left\{\sum_{i=1}^{N_{\text{rw}}} \mathcal{P}_i + \sum_{i=1}^{N_{\text{rw}}} (z_{a,i} + z_{b,i})\right\} dt \\
\text{Subject To:} & \\
 & \begin{bmatrix} \dot{q} \\ \dot{\omega} \\ \dot{\Omega}_{rw} \end{bmatrix} = \begin{bmatrix} \frac{1}{2}\mathcal{Q}(\omega) q \\ J_{\text{sc}}^{-1}(AA^{+}\tau_{\text{sc}}^{\mathcal{B}} - \omega \times (J_{\text{sc}}\omega + AJ_{\text{rw}}\Omega_{\text{rw}})) \\ -J_{\text{rw}}^{-1}A^{+}\tau_{\text{sc}}^{\mathcal{B}} \end{bmatrix} \\
 & x(0) = \left[q^0,\ \omega^0,\ \Omega_{\text{bias}}\right]^{\mathsf{T}} \in \mathbb{R}^{7+N_{\text{rw}}} \\
 & x(t_f) = \left[q^f,\ \omega^f,\ \Omega_{\text{bias}}\right]^{\mathsf{T}} \in \mathbb{R}^{7+N_{\text{rw}}} \\
 & z_{a,i} \geq 0,\ \forall\, i = 1, \ldots, N_{\text{rw}} \\
 & z_{b,i} \geq 0,\ \forall\, i = 1, \ldots, N_{\text{rw}} \\
 & z_{a,i} - \mathcal{P}_i \geq 0,\ \forall\, i = 1, \ldots, N_{\text{rw}} \\
 & z_{b,i} + \mathcal{P}_i \geq 0,\ \forall\, i = 1, \ldots, N_{\text{rw}} \\
 & |\omega_i| \leq \omega_{\max},\ \forall\, i = 1, 2, 3 \\
 & |\Omega_{rw,i}| \leq \Omega_{\max},\ \forall\, i = 1, \ldots, N_{\text{rw}} \\
 & \left|(A^{+}\tau_{\text{sc}}^{\mathcal{B}})_i\right| \leq \tau_{\max},\ \forall\, i = 1, \ldots, N_{\text{rw}}
\end{cases}
$$

The increase in dimensionality needed to obtain the equivalent *smooth* formulation to problem A_{ns} is to add $2N_{\text{rw}}$ (ancillary) control variables, along with $4N_{\text{rw}}$ constraints (thereby bringing the total path constraints in problem A_{ns} to $6N_{\text{rw}}+3$). While there is a computational-cost for increasing the dimensionality to the optimal control problem A_{ns}, it allows the *original* problem to directly be solved without having to resort to information loss, either through resorting to proxies to the cost functional, linearizing the dynamics, or through homotopic approaches in which a sequence of problems are solved which converge to a solution to the original problem. Problem A_s may be readily solved numerically using any of the standard computational optimal control algorithms. Additionally, Pontryagin's Minimum Principle may be directly applied to problem A_s to obtain necessary conditions for optimality. In this paper, problem A_s is numerically solved utilizing the software-package DIDO, which implements pseudospectral optimal control theory (see Refs. [18,20,21,42]).

Problem A_s when populated with the real world spacecraft parameters from the Appendix, is almost certainly a poorly conditioned problem. Therefore to try to obtain an numerical solution to problem A_s in its presented form is ill-advised as it would be quite challenging if not impossible. Rather, designer units[19,43] should be invoked to generate an equivalent problem $\overline{A_s}$. Then solutions to problem $\overline{A_s}$ may be de-scaled to obtain a solution to the original problem A_s. For a thorough treatment of the subject, the reader is directed to the references [19] and [43]. The numerical solutions obtained and presented in this paper to problem A_s had scaling through designer-units performed upon each state and control variable. Additionally scaling was performed upon each path constraint. The details are omitted for brevity

Necessary Conditions for Optimality

In this section, the necessary conditions for optimality for problem A_s are obtained through the application of Pontryagin's Minimum Principle. Necessary conditions serve an important role in the validation of a numerical solution, serving as a fail-test for potential solutions to problem A_s. At the heart of Pontryagin's Minimum Principle is the Hamiltonian Minimization Condition (HMC). The HMC states that, for an extremal control u^* to be optimal, it necessarily must minimize the control Hamiltonian at each instant of time. Due to the presence of state and control path constraints in problem A_s the necessary conditions from the HMC are obtained by applying the Karush-Kuhn-Tucker (KKT) conditions through the consideration of the Lagrangian of the control Hamiltonian:

$$\overline{H}(\mu, \lambda, x, u) = H(\lambda, x, u) + \mu^{\mathsf{T}} h(x, u) \tag{18}$$

where $H(\lambda, x, u) \in \mathbb{R}$ is the control Hamiltonian, $\mu \in \mathbb{R}^{3+6N_{\text{rw}}}$ the path covector consisting of the KKT multipliers associated to the HMC, and $h \in \mathbb{R}^{3+6N_{\text{rw}}}$ the vector of path constraints. By the KKT conditions,

at each instant of time, the Lagrangian of the Hamiltonian must necessarily be stationary with respect to the control u:

$$\frac{\partial \overline{H}}{\partial u} = \frac{\partial \overline{H}}{\partial u} + \left(\frac{\partial h}{\partial u}\right)^{\intercal} \mu = 0 \in \mathbb{R}^{3+2N_{\text{rw}}} \tag{19}$$

Along with the stationary condition, the KKT conditions require the path covectors and path constraints satisfy the complementarity conditions: For each $i = 1, \ldots, 3 + 6N_{\text{rw}}$

$$\mu_i \begin{cases} \geq 0 & \text{if } h_i(x,u) = h_i^U \\ = 0 & \text{if } h_i^L < h_i(x,u) < h_i^U \\ \leq 0 & \text{if } h_i(x,u) = h_i^L \end{cases} \tag{20}$$

To simplify the presentation of the necessary conditions of problem A_{s}, the minimization of $\mathcal{E}$ is rewritten as it is equivalent to the minimization of the following cost functional:

$$J_{\text{equiv}}\left[x(\cdot), u(\cdot)\right] = \int_0^T \sum_{i=1}^{N_{\text{rw}}} \left(\frac{R}{K_\tau^2}\right) \tau_{\text{rw},i}^2 + \left(\frac{R\beta_{\text{v}}}{K_\tau^2} + 1\right) \beta_{\text{v}} \Omega_{\text{rw},i}^2 + (z_{a,i} + z_{b,i})\, dt. \tag{21}$$

The equivalency of the cost functional in Eq. (21) to that in Problem A_{s} is by the invariance of minimization under scalar multiplication and under vertical translations, along with the following relationship[9]

$$\int_0^T \sum_{i=1}^{N_{\text{rw}}} \tau_{\text{rw},i}(t) \Omega_{\text{rw},i}(t)\, dt = \sum_{i=1}^{N_{\text{rw}}} \frac{J_{\text{rw},i}}{2} \left(\Omega_{\text{rw},i}^2(T) - \Omega_{\text{rw},i}^2(0)\right), \tag{22}$$

which is arrived through Eq. (4). The control Hamiltonian for problem A_{s} is therefore given by

$$\begin{aligned} H(\lambda, x, u) = \sum_{i=1}^{N_{\text{rw}}} \left(\left(\frac{R}{K_\tau^2}\right) \tau_{\text{rw},i}^2 + \left(\frac{R\beta_{\text{v}}}{K_\tau^2} + 1\right) \beta_{\text{v}} \Omega_{\text{rw},i}^2 + (z_{a,i} + z_{b,i}) \right) + \lambda_q^{\intercal} \left(\frac{1}{2} \mathcal{Q}(\omega) q\right) \\ + \lambda_\omega^{\intercal} \left(J_{\text{sc}}^{-1} (A A^{+} \tau_{\text{sc}}^{\mathcal{B}} - \omega \times (J_{\text{sc}} \omega + A J_{\text{rw}} \Omega_{\text{rw}}))\right) + \lambda_\Omega^{\intercal} \left(-J_{\text{rw}}^{-1} A^{+} \tau_{\text{sc}}^{\mathcal{B}}\right), \end{aligned} \tag{23}$$

where each $\lambda_q \in \mathbb{R}^4, \lambda_\omega \in \mathbb{R}^3, \lambda_\Omega \in \mathbb{R}^{N_{\text{rw}}}$, is a vector of costates with subscript corresponding to the associated state variable vector. The Lagrangian of the (control) Hamiltonian, is given by

$$\begin{aligned} \overline{H}(\mu, \lambda, x, u) = H(\lambda, x, u) + \mu_a^{\intercal} z_a + \mu_b^{\intercal} z_b + \sum_{i=1}^{N_{\text{rw}}} \mu_{pos,i} (z_{a,i} - \mathcal{P}_i) + \sum_{i=1}^{N_{\text{rw}}} \mu_{neg,i} (z_{b,i} + \mathcal{P}_i) \\ + \mu_\omega^{\intercal} \omega + \mu_\Omega^{\intercal} \Omega + \mu_\tau^{\intercal} \left(A^{+} \tau_{\text{sc}}^{\mathcal{B}}\right) \end{aligned} \tag{24}$$

where each $\mu_a, \mu_b, \mu_{pos}, \mu_{neg}, \mu_\Omega, \mu_\tau \in \mathbb{R}^{N_{\text{rw}}}, \mu_\omega \in \mathbb{R}^3$, is a vector of KKT covectors with subscript corresponding to the associated vector of path constraints. While Eq. (24) is somewhat lengthy, expressions for the stationary conditions in Eq. (19) may be attained through a straightforward application of matrix calculus:

$$0 = \frac{\partial \overline{H}}{\partial \tau_{\text{sc}}^{\mathcal{B}}} = \left(\lambda_\omega^{\intercal} J_{\text{sc}}^{-1} A A^{+}\right)^{\intercal} - \left(\lambda_\Omega^{\intercal} J_{\text{rw}}^{-1} A^{+}\right)^{\intercal} + \left(\mu_\tau A^{+}\right)^{\intercal} \tag{25}$$

$$0 = \frac{\partial \overline{H}}{\partial z_{a,i}} = 1 + \mu_{a,i} + \mu_{pos,i} \qquad \forall i = 1, \ldots, N_{\text{rw}} \tag{26}$$

$$0 = \frac{\partial \overline{H}}{\partial z_{b,i}} = 1 + \mu_{b,i} + \mu_{neg,i} \qquad \forall i = 1, \ldots, N_{\text{rw}} \tag{27}$$

While the KKT conditions require that each of the seven collections of KKT covectors making up μ have associated to them complementarity conditions, for the sake of brevity, only μ_a and μ_ω are presented as the

the rest follow in like manner:

$$\mu_{\omega,i}\begin{cases}\geq 0 \ \text{ if } \omega_i = \omega_{\max} \\ = 0 \ \text{ if } -\omega_{\max} < \omega_i < \omega_{\max} \\ \leq 0 \ \text{ if } \omega_i = -\omega_{\max}\end{cases}, \qquad \mu_{a,j}\begin{cases}= 0 \ \text{ if } 0 < z_{a,j} < \infty \\ \leq 0 \ \text{ if } z_{a,j} = 0\end{cases} \tag{28}$$

Along with the complementarity conditions and stationary conditions, another extremely important necessary condition for the validation of numerically computed solution is arrived upon by considering the lower Hamiltonian and how it evolves over time. The lower Hamiltonian, $\mathcal{H}$, is acquired by evaluating the (control) Hamiltonian along an extremal solution, u^*, of the HMC, i.e. $\mathcal{H}(\lambda, x) \triangleq H(\lambda, x, u^*)$, and evolves over time according to $\dot{\mathcal{H}}(\lambda, x) = \partial_t \overline{H}$ (known as the Hamiltonian Evolution Equation [19]). Therefore, because problem A_s is time invariant, the Hamiltonian Evolution Equation states that optimal solutions to problem A_s must necessarily have lower Hamiltonian which is constant for all time, i.e.

$$\frac{d}{dt}\mathcal{H}(\lambda, x) = 0 \qquad \forall\, t \in [0, T]. \tag{29}$$

The use of the adjoint equations to problem A_s, which evolve according to $-\dot{\lambda} = \partial_x \overline{H}$, for the purpose of validating numerical solutions of problem A_s is not helpful because the equations are complicated. For example, the adjoint associated to the quaternions evolve according to

$$\begin{aligned}
\dot{\lambda}_{q_1} &= \tfrac{1}{2}\left(\lambda_{q_2}\omega_3 - \lambda_{q_2}\omega_2 + \lambda_{q_4}\omega_1\right) \\
\dot{\lambda}_{q_2} &= \tfrac{1}{2}\left(-\lambda_{q_1}\omega_3 + \lambda_{q_3}\omega_1 + \lambda_{q_4}\omega_2\right) \\
\dot{\lambda}_{q_3} &= \tfrac{1}{2}\left(\lambda_{q_1}\omega_2 - \lambda_{q_2}\omega_1 + \lambda_{q_4}\omega_3\right) \\
\dot{\lambda}_{q_4} &= \tfrac{1}{2}\left(-\lambda_{q_1}\omega_1 - \lambda_{q_2}\omega_2 - \lambda_{q_3}\omega_3\right)
\end{aligned}$$

Therefore, the necessary conditions used in this paper to demonstrate the validity of a numerical solution for optimality include the stationary conditions, complimentary conditions, and the consistency of the lower Hamiltonian.

Along with verifying the satisfaction of the necessary conditions for the candidate optimal control solution it is also necessary to demonstrate the feasibility of the candidate optimal control, u^*. This feasibility analysis is carried out by propagating u^* through the dynamics using a standard Runge-Kutta (RK) integrator. The candidate optimal control is deemed feasible if and only if the solution returned by the RK integrator coincides with the solution obtained by the numerical solver, to within a predefined tolerance, i.e. $\epsilon < 10^{-6}$ where ϵ is the error. For an in depth discussion on the verification and validation of optimal control solutions, see Ross [19]. All results present in this paper successfully passed feasibility within the predefined tolerance specified in this section.

MINIMUM ENERGY ATTITUDE STEERING

This section demonstrates the existence and efficacy of minimum energy rest-to-rest slews by steering the attitude of a spacecraft which implements its own control allocation scheme (thereby precluding the direct control of the motor toques generated by the reaction wheels). The spacecraft is assumed to distribute the control torque through a least-squares allocation scheme (i.e. Moore-Penrose). To demonstrate the minimum energy attitude steering maneuver, a 180-degree rest-to-rest slew about the spacecraft's z-axis is considered, whose initial and final quaternions are $q^0 = [0, 0, 1, 0]^\intercal$ and $q^f = [0, 0, 0, 1]^\intercal$ and parameters are given in the Appendix.

Baseline Eigenaxis Maneuver

The maneuver type which serves as the baseline is a conventional shortest time eigenaxis maneuver (ST-EAM) under least-squares control allocation. In order to obtain the ST-EAM under L^2 allocation, a problem formulation is constructed and solved which is analogous to A_{ns}: (*i*) Replace the cost functional with transfer

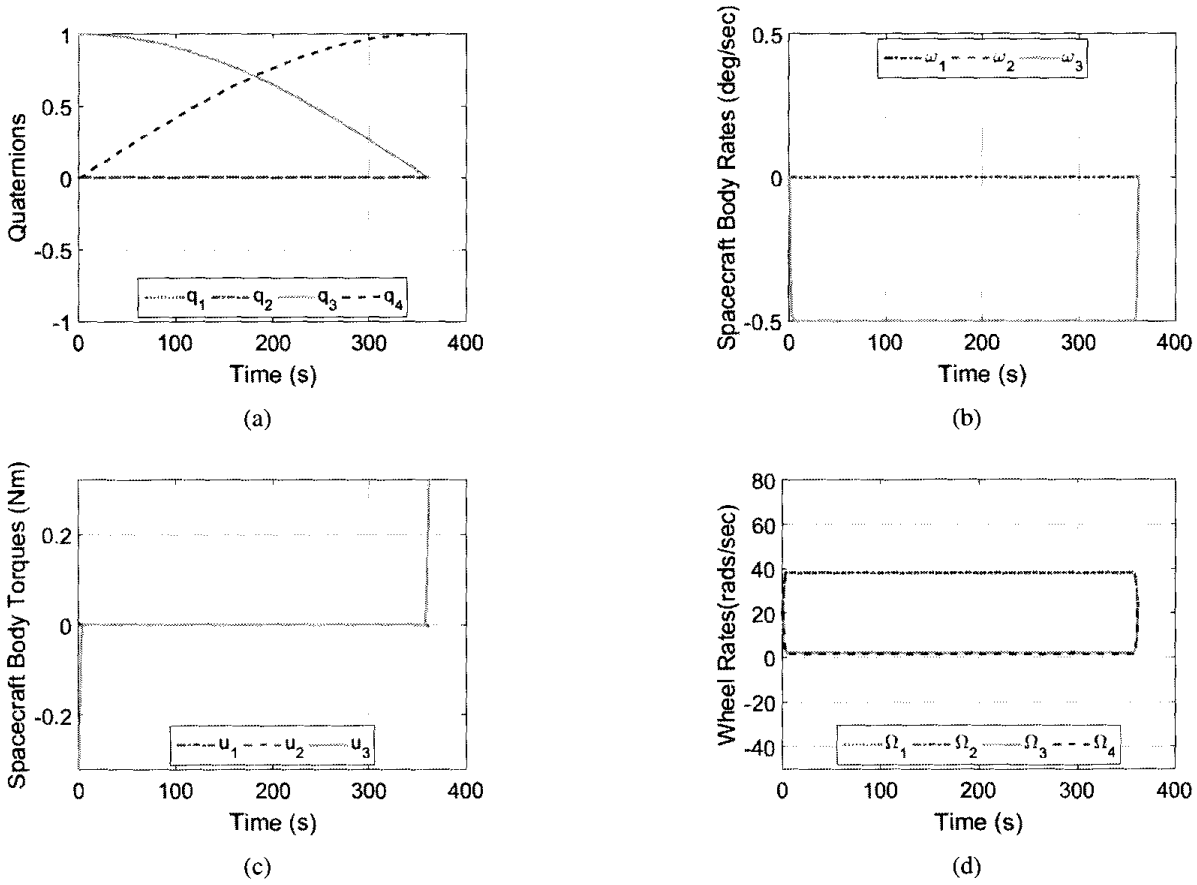

Figure 1: State and control profiles of a Shortest Time Eigenaxis Maneuver for a 180-deg rest-to-rest slew about the spacecraft z-axis: (a) attitude; (b) body rates; (c) body torques (control); (d) reaction wheel rates.

time, i.e. $J[x(\cdot), u(\cdot), t_f] = t_f$, (*ii*) Add the path constraint in Eq. (13) which enforces eigenaxis maneuvering, and (*iii*) Incorporate the spherical slew rate constraint $\|w\|_2 \leq \omega_{\max}$ and remove the path constraint $|\omega_i| < \omega_{\max}$ for each $i = 1, 2, 3$.

The shortest-time eigenaxis maneuver to the 180-degree slew completes in 362.0 seconds, and requires 108 J of energy. The state and control profiles associated to the ST-EAM are shown in Figure 1. Pontryagin's Minimum Principle states that the lower Hamiltonian should be -1 over the entire time horizon for minimum-time problems, and Figure 4a depicts the consistency of the lower Hamiltonian associated to the solution. The monotonicity of the quaternions in Figure 1a depict that the obtained solution is in fact an eigenaxis maneuver. Figure 1b shows the build up of the angular velocity of the spacecraft is about the z-axis (the eigenaxis for this particular maneuver). The control profile seen in Figure 1c is bang-bang, which is consistent for shortest time maneuvers. The reaction wheel speeds seen in Figure 1d are observed to begin and end the maneuver at their specified biases of 20 rad/sec.

By solving problem A_s, with the upper bound on transfer time to be the slew time for the baseline eigenaxis maneuver, i.e. $T = 362.0$ seconds, a minimum energy maneuver is obtained by steering the attitude of the spacecraft and hence working about the ACS which allocates the control toque through a least-squares scheme. The solution obtained solving A_s completes the slew with the same transfer time as the baseline eigenaxis maneuver, yet requires 36.4% less energy (69.1 J as compared to 108.1 J). The state and control profiles to this minimum energy solution is given in Figure 2, and differ dramatically from the state and control profiles obtained by solving for the baseline eigenaxis maneuver. Problem A_s does not restrict motion to be along the eigenaxis, and so off-eigenaxis maneuvering is feasible to problem A_s. The non-monotonicity of the quaternion attitude profiles in Figure 2a demonstrates that the minimum energy attitude steering maneuver

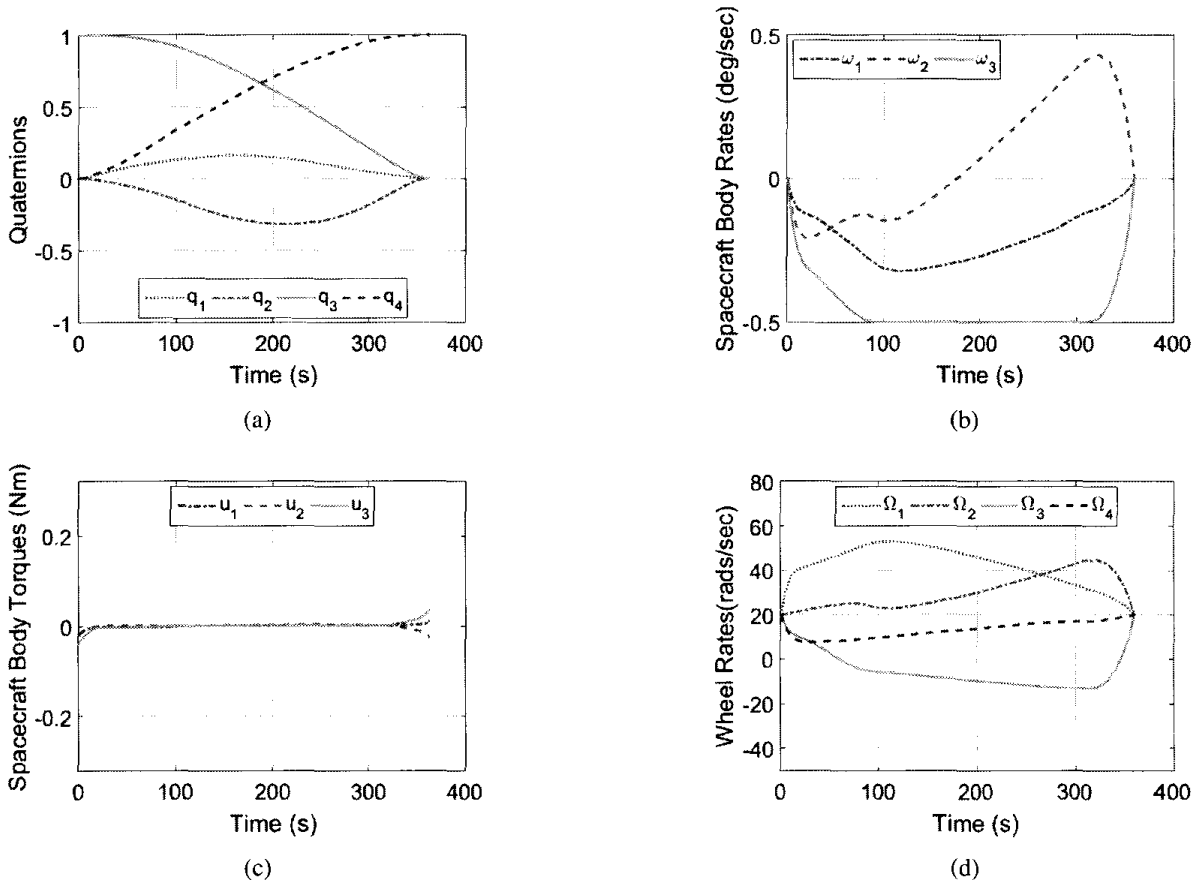

Figure 2: State and control profiles of a Minimum Energy Attitude Steered Maneuver, for a 180-deg rest-to-rest slew about the spacecraft z-axis: (a) attitude; (b) body rates; (c) body torques; (d) reaction wheel rates.

utilizes off-eigenaxis maneuvering to complete the slew. Off-eigenaxis maneuvering allows the spacecraft

Table 1: Metrics to the baseline eigenaxis maneuver in Figure 1, and the minimum energy attitude steering maneuver in Figure 2 (values in parenthesis represent percentage change from the baseline).

Maneuver Type	TT (s)	$\mathcal{E}$ (J)	$\mathcal{E}_{total}^{loss}$ (J)	$\mathcal{C}_{loss}$ (J)	$\mathcal{F}_{loss}$ (J)
Shortest Time Eigenaxis Maneuver	362.0	108.7	106.3	61.1	45.2
Minimum Energy Attitude Steering	362.0 (0.0%)	69.1 (-36.4%)	56.4 (-46.9%)	8.2 (-86.6%)	48.3 (+6.9%)

to build the body-velocities simultaneously about each its axes, with saturation about the spacecraft z-axis from 85 seconds to 310 seconds, as seen in Figure 2b Figures 2c and 2d depict the control (spacecraft body torque) and the reaction wheel speeds. Comparing the torques of the minimum energy maneuver to those from the conventional baseline eigenaxis maneuver, the bang-bang profiles are now replaced with markedly less-demanding control profiles. This difference in torque authority translates into an 87% reduction in copper loss from the baseline eigenaxis maneuver (from 61.1 J to 8.2 J). The speed profile to each reaction wheel for the minimum energy maneuver is given in Figure 2d. On account of the effort towards maneuvering off-eigenaxis, the friction loss incurred by the minimum energy attitude steered maneuver increases by 7% from the conventional EAM (45.2 J to 48.3 J). Even with the small increase in frictional losses, the minimum energy steered solution reduces the dissipative losses by 47% (56.4 J as compared to 106.3), and therefore has less heat to reject than the canonical EAM. Table 1 summarizes the slew-time and energy metrics between the conventional EAM and the minimum energy solution. To demonstrate the efficacy by which minimum en-

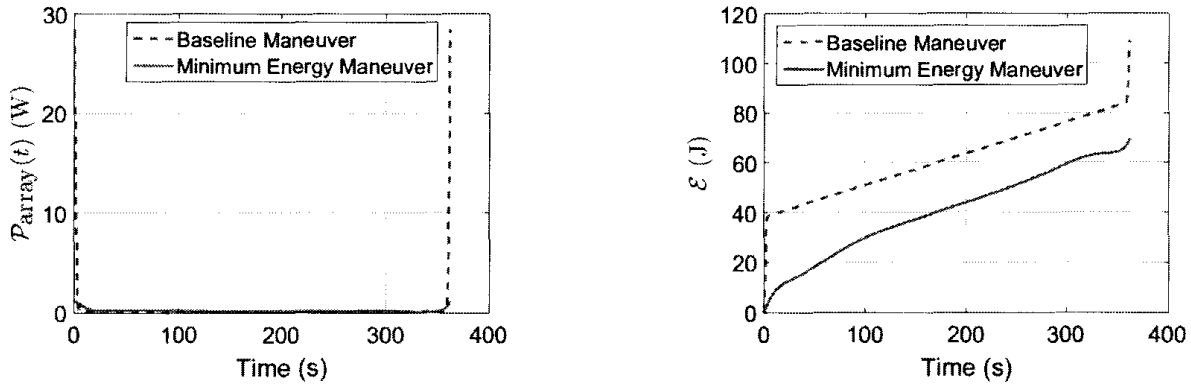

Figure 3: Comparison between the baseline eigenaxis maneuver and minimum energy attitude steering: (a) Electrical power consumed by the RWA; (b) Cumulative electrical energy consumed by the RWA.

ergy attitude steered solutions reduce power requirements, the time histories of power and cumulative energy consumed by the reaction wheel array for the solution to problem A_s is compared against the baseline eigenaxis maneuver, and are given in Figure 3. In the comparison of RWA power usage, Figure 3a shows that the minimum-energy solution reduces the peak power demand by nearly 96% (from 28.3 W to 1.2 W), average power by 85% (from 2.0 W to 0.3 W), thereby reducing the peak-to-average power ratio by 76% (from 14.5 to 3.5). Table 2 summarizes the comparison of peak and average power between the two maneuver schemes. In Figure 3b, the total energy consumption of the RWA for the two maneuver schemes is shown. It is clear that by steering the attitude of the spacecraft, the energy required to perform the slew is substantially reduced and that *enforcing eigenaxis maneuvering limits the spacecraft with respect to energy.*

Table 2: Reaction wheel array power usage of the baseline eigenaxis maneuver compared to the minimum energy attitude steered maneuver (values in parenthesis represent percentage change from the baseline).

Maneuver Type	Peak Power (W)	Average Power (W)	Peak-to-Average Power Ratio
Shortest Time Eigenaxis Maneuver	28.3	2.0	14.5
Minimum Energy Attitude Steering	1.2 (-95.8%)	0.3 (-85.0%)	3.9 (-73.1%)

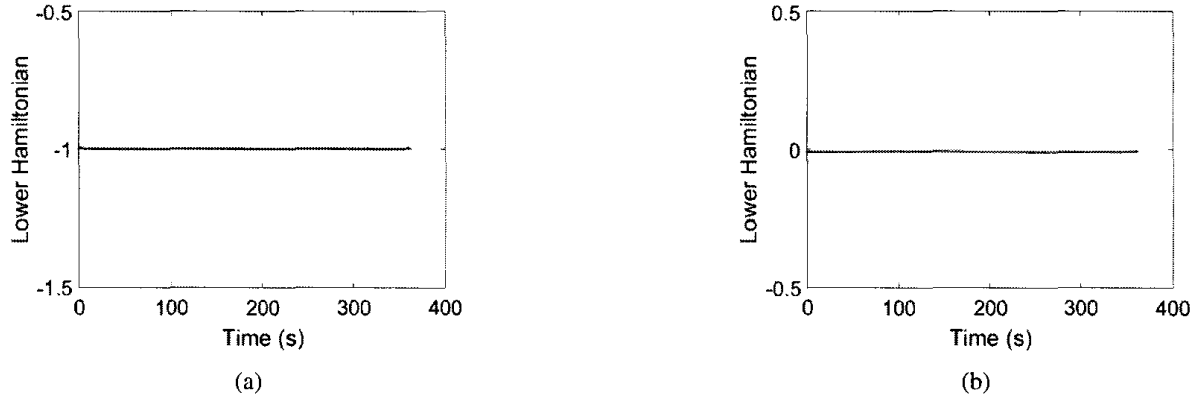

Figure 4: Consistency of the lower Hamiltonian for the: (a) ST-EAM ; (b) minimum energy attitude steering.

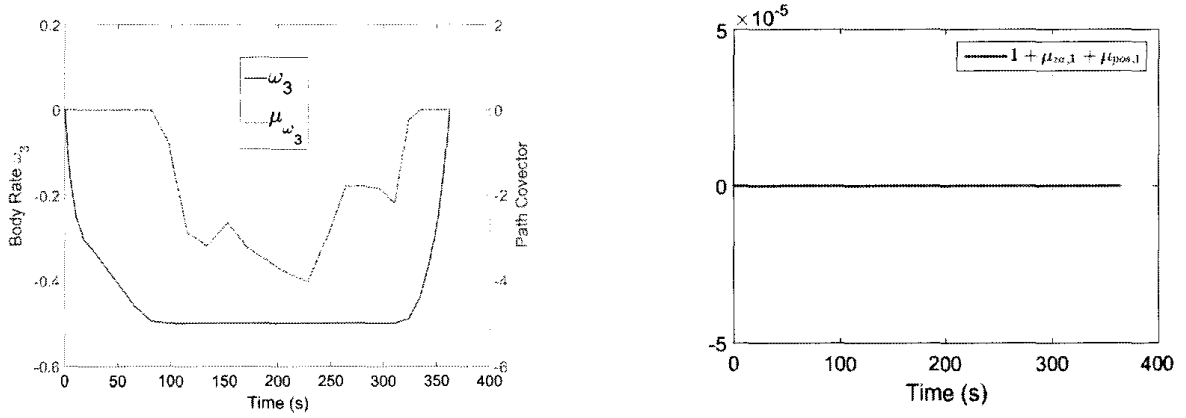

(a) Complementarity condition (b)

Figure 5: Verification of necessary conditions to the Minimum Energy Attitude Steered 180-deg rest-to-rest slew about the spacecraft z-axis: (a) Complementarity condition for ω_3; (b) Stationary condition for $z_{a,1}$.

Lastly, the minimum-energy solution obtained from solving problem A_s is to be vetted against the necessary conditions of optimality. Figures 4b and 5 show the the numerical solution obtained from solving problem A_s satisfies the necessary conditions given by Pontryagin's Minimum principle. The (lower) Hamiltonian associated to the numerical solution obtained by solving the minimum energy maneuver is shown in Figure 4b, and is consistent with the Hamiltonian Evolution Equation of Pontryagin's Minimum Principle, which requires that the Hamiltonian be a fixed constant for all time over the finite horizon $[0, T]$. While the Hamiltonian associated to the minimum energy solution is demonstrated to be constant, it is not -1; this discrepancy is due to the fact that problem A_s is solved as a *fixed-time* problem, not a *minimum-time* problem. Figure 5a shows the complementarity condition on the spacecraft angular rate, ω_3: The KKT multiplier associated to ω_3 is observed to vary in accordance to Eq. (28) which specifies that $\mu_{\omega,3} = 0$ unless the constraint upon ω_3 is active. The specifics on the other necessary conditions such as the details on transversality, the Hamiltonian value conditions, etc. while verified, have been omitted for brevity. Therefore, by passing both feasibility and the necessary conditions posed by Pontryagin's Minimum Principle, the solution obtained by solving to problem A_s may be considered an optimal solution.

FEEDBACK IMPLEMENTATION

In a practical flight setting, the open-loop control-laws that are obtained solving optimal control problems are not flown. This is due to the certain presence of system uncertainty (e.g. from sensor or the inertia tensor). Therefore, in a practical flight setting, slews must be executed in closed-loop. In this section, the attitude and body rate trajectories associated to the baseline eigenaxis maneuver and the minimum energy attitude steering used as inputs to a standard quaternion-error control-law. A block diagram of the control loop is shown in Figure 6. Figure 7 shows that the feedback controller correctly tracks the attitude and body rate of the

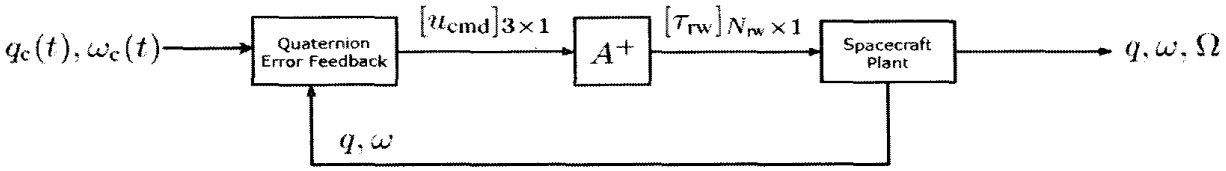

Figure 6: Quaternion error feedback control law for implementing minimum energy maneuvers

two maneuvers. Tables 3 and 4 summarize the energy and power performance due to tracking the baseline eigenaxis maneuver, as well as the minimum energy maneuver, obtained by solving to Problem A_s. The small discrepancy in the energy and power metrics between the open-loop and closed-loop performances for both

maneuver schemes, is in part because the influence from the dynamics of the ACS were not considered in the problem formulations for either maneuver type. Even with this small discrepancy, by opting for the minimum energy maneuver over the baseline shortest time eigenaxis maneuver, the slew may be completed with 36% less energy (from 113.1 J to 72.2 J) with dissipative losses reduced by 46% (from 109.0J to 59.4 J). The minimum energy off-eigenaxis maneuver is able to drive the peak-to-average power ratio down from 81.4 to 6.5 (a reduction of 92%), completing the baseline maneuver with 95% less peak power (1.2 W as compared to 23.0 W). Figures 8 and 9 depicts the stark difference in energy and power consumption between the two maneuver schemes and demonstrate that the open-loop solutions accurately predict the closed-loop response of the feedback controller in Figure 6.

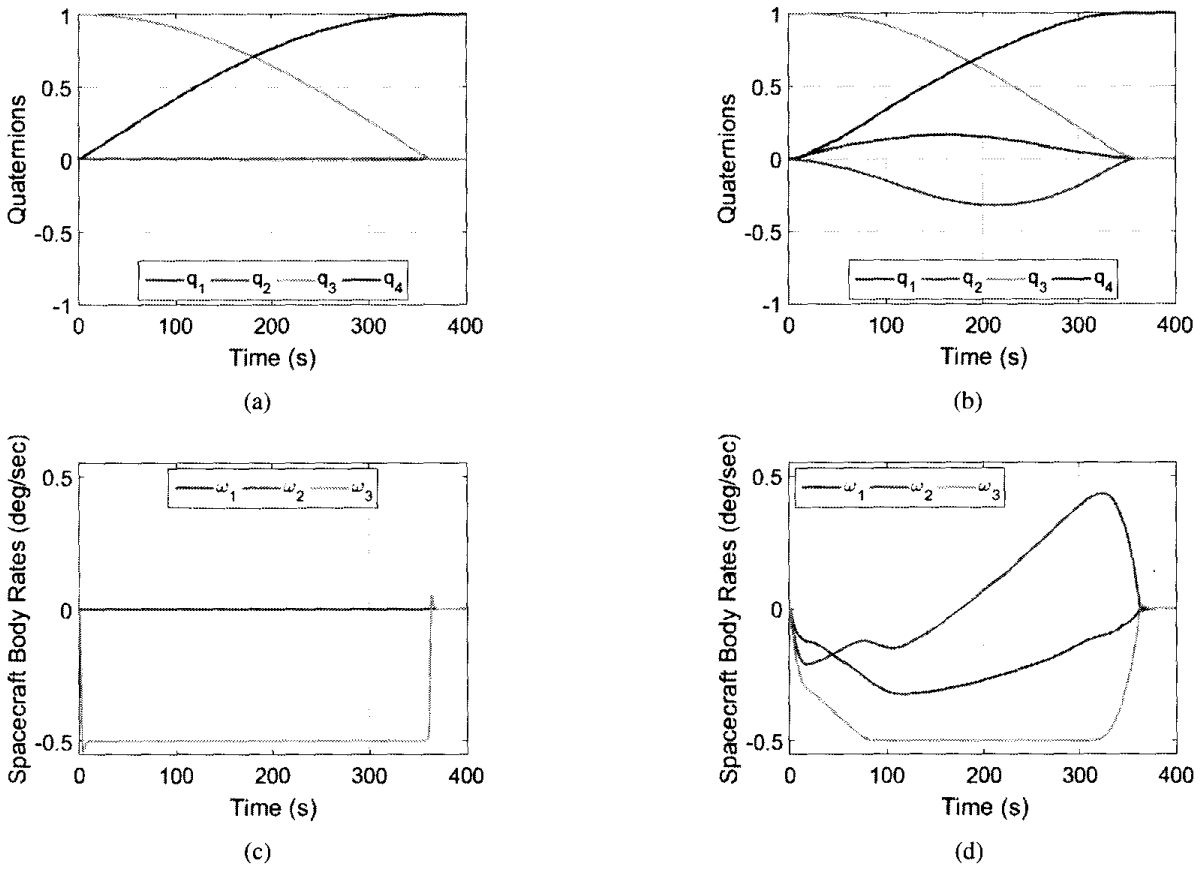

Figure 7: Closed-loop state profiles for the baseline eigenaxis maneuver and minimum energy attitude steering: baseline attitude and body rates in (a) and (c) ; attitude and body rates for minimum energy attitude steering in (b) and (d).

Table 3: Metrics to the close-loop implementation of the baseline eigenaxis maneuver and minimum energy attitude steering in Figure 7 (values in parenthesis represent percentage change from tracking the baseline).

Maneuver Type	TT (s)	$\mathcal{E}$ (J)	$\mathcal{E}_{total}^{loss}$ (J)	$\mathcal{C}_{loss}$ (J)	$\mathcal{F}_{loss}$ (J)
Baseline Eigenaxis Maneuver	400.0	113.1	109.0	61.1	47.9
Minimum Energy Attitude Steering	400.0 (0.0%)	72.2 (36.2%)	59.4 (-45.5%)	8.0 (-86.9%)	51.4 (+7.3%)

Table 4: RWA power usage to the closed-loop the baseline eigenaxis maneuver and minimum steering (values in parenthesis represent percentage change from the closed-loop baseline).

Maneuver Type	Peak Power (W)	Average Power (W)	Peak-to-Average Power Ratio
Baseline Eigenaxis Maneuver	23.0	0.3	81.4
Minimum Energy Attitude Steering	1.2 (-94.8%)	0.2 (-33.3%)	6.5 (-92.0%)

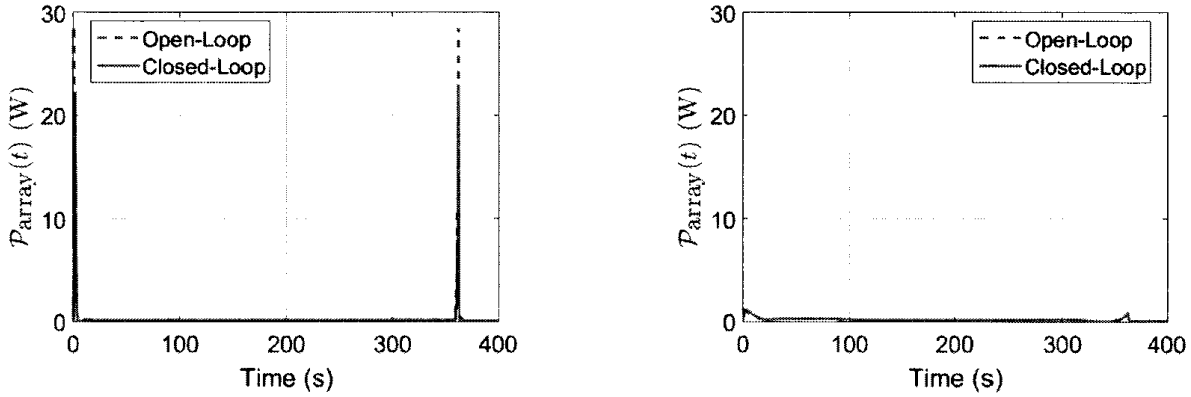

(a) (b)

Figure 8: Power consumed by the reaction wheel array over the maneuver for the open-loop (dashed) and closed-loop (solid) implementation: (a) baseline eigenaxis maneuver; (b) minimum energy attitude steering.

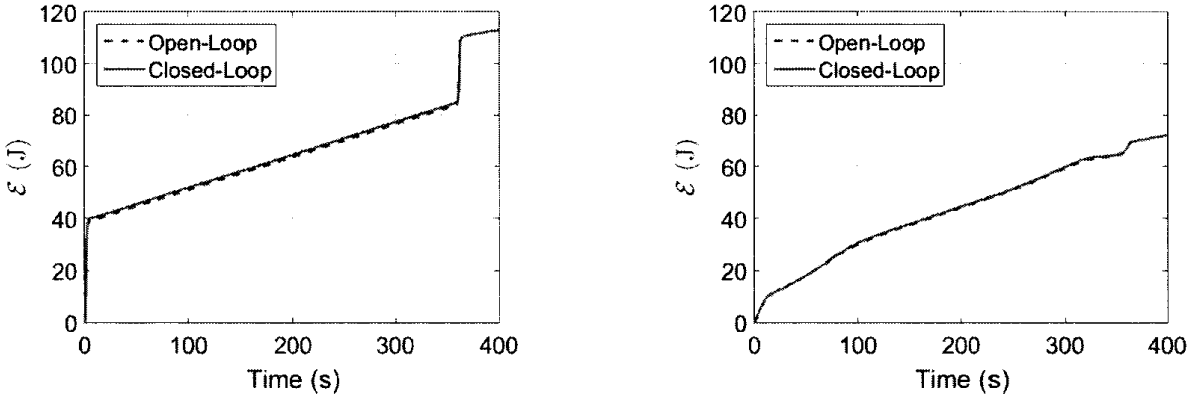

(a) (b)

Figure 9: Energy for open-loop (dashed) and closed-loop (solid) implementation: (a) baseline eigenaxis maneuver; (b) minimum energy attitude steering.

CONCLUSIONS

This paper demonstrates the existence of solutions to minimum electrical energy maneuvering in the situations *when the reaction wheels can not be directly controlled*, such as with a heritage attitude control system. The approach taken was the formulation of a family of nonlinear nonsmooth L^1, operationally relevant, optimal control problems to minimize the electrical energy the reaction wheel array to perform a slew, *solely* through steering the attitude of the spacecraft. Steering the attitude can produce maneuvers which substantially reduced electrical energy requirements (a decrease of 36%), and dramatically reduce peak power (a decrease of 95%), as compared to conventional eigenaxis maneuvering. Results present in this paper demonstrate that *a significant penalty to both energy and power is incurred by enforcing eigenaxis maneuvering*. By maneuvering off-eigenaxis, energy, dissipative losses, and peak power are dramatically reduced. Therefore, late in the mission life of a spacecraft, when diminished power profiles are more likely to occur, more slews may be feasible by opting for minimum energy maneuvering in situations where the reaction wheels can not be directly controlled.

Additionally it was shown that the open-loop solutions for minimum energy attitude steering can be implemented using closed-loop control. Moreover the open-loop solutions accurately predict the closed loop response. Therefore in situations where the ACS does not permit direct access to the reaction wheels, attitude steering may be utilized as a valuable tool for managing power and energy requirements. Additionally it is noted that no modification to the flight software is required to fly the new minimum energy maneuvers. Because of this, there is a great potential to effect and implement these reduced energy maneuvers on a broad class of spacecraft.

APPENDIX

The parameters for the example spacecraft used throughout this paper are summarized in Table 5.

Parameter Description	Symbol	Value & Units
Armature resistance	R	1.8 Ohms
Motor torque constant	K_{T}	0.0696 Nm/A
Back EMF constant	K_{V}	0.0696 V $\cdot$ (rads/s)$^{-1}$
Wheel viscous friction coefficient	β_{v}	4.3×10^{-5} Nm $\cdot$ (rads/s)$^{-1}$
Maximum reaction wheel speed	$\Omega_{\max}$	450.0 rads/s
Maximum motor torque	$\tau_{\max}$	0.14 Nm/s
Wheel rotor inertia	J_{rw}	0.012 kg $\cdot$ m^2
Wheel speed bias	Ω_{bias}	20.0 rads/s
Rate gyro limit	$\omega_{\max}$	0.5 degs/s – per axis
Reaction wheel projection matrix	A	$\frac{1}{\sqrt{3}}\begin{bmatrix} 1 & -1 & -1 & 1 \\ 1 & -1 & 1 & -1 \\ 1 & 1 & -1 & -1 \end{bmatrix}$
Spacecraft inertia tensor	J_{sc}	$\begin{bmatrix} 59.22 & -1.14 & -0.80 \\ -1.14 & 40.56 & 0.10 \\ -0.80 & 0.10 & 57.60 \end{bmatrix}$ kg $\cdot$ m^2

Table 5: Spacecraft parameters [32, 37, 46] used in this work.

REFERENCES

[1] N. Dennehy, "Spacecraft Hybrid Control at NASA: A Look Back, Current Initiatives, and Some Future Considerations," *Proceedings of the 37th Annual AAS Guidance and Control Conference*, No. AAS paper: AAS-14-101., Breckenridge, CO, January 31 – February 5, 2014 2015.

[2] A. Y. Lee and E. K. Wang, "In-Flight Performance of Cassini Reaction Wheel Bearing Drag in 19972013," *Journal of Spacecraft and Rockets*, Vol. 52, Jan. 2015, pp. 470–480, 10.2514/1.A33047.

[3] D. J. Sahnow, H. W. Moos, S. D. Friedman, W. P. Blair, S. J. Conard, J. W. Kruk, E. M. Murphy, W. R. Oegerle, and T. B. Ake III, "Far Ultraviolet Spectroscopic Explorer: one year in orbit," *International Symposium on Optical Science and Technology*, International Society for Optics and Photonics, 2000, pp. 131–136.

[4] L. E. Bell, "Cooling, heating, generating power, and recovering waste heat with thermoelectric systems," *Science*, Vol. 321, No. 5895, 2008, pp. 1457–1461.

[5] A. Witze, "Desperately Seeking Plutonium," *Nature*, Vol. 515, No. 7528, 2014, p. 484.

[6] S. M. Krimigis and R. B. Decker, "The Voyagers' Odyssey," *American Scientist*, Vol. 103, No. 4, 2015, p. 284.

[7] W. H. Larson and J. L. e. Wertz, "Space Mission Analysis and Design, 3rd ed.," *Space Mission Analysis and Design, 3rd ed.*, p. 369, Portland, OR: Microcosm Press, 1999.

[8] M. Karpenko, C. J. Dennehy, H. C. Marsh, and Q. Gong, "Minimum Power Slews and the James Webb Space Telescope," *27th AAS/AIAA Space Flight Mechanics Meeting*, No. Paper number: AAS 17-285, San Antonio, TX, February 5 to February 9 2017.

[9] H. Marsh, M. Karpenko, and Q. Gong, "Energy Constrained Shortest-Time Maneuvers For Reaction Wheel Satellites," *AIAA/AAS Astrodynamics Specialist Conference*, 2016, p. 5579.

[10] W. R. Wehrend, "Minimum Energy Reaction Wheel Control for a Satellite Scanning a Small Celestial Area," NASA TN D-392, 1967.

[11] S. Skaar and L. Kraige, "Single-Axis Spacecraft Attitude Maneuvers Using an Optimal Reaction Wheel Power Criterion," *Journal of Guidance, Control, and Dynamics*, Vol. 5, No. 5, 1982, pp. 543–544.

[12] S. Skaar and L. Kraige, "Large-Angle Spacecraft Attitude Maneuvers Using an Optimal Reaction Wheel Power Criterion," *Journal of the Astronautical Sciences*, Vol. 32, No. 1, 1984, pp. 47–61.

[13] H. Schaub and V. J. Lappas, "Redundant Reaction Wheel Torque Distribution Yielding Instantaneous L2 Power-Optimal Spacecraft Attitude Control," *Journal of Guidance, Control, and Dynamics*, Vol. 32, No. 4, 2009, pp. 1269–1276.

[14] R. Blenden and H. Schaub, "Regenerative Power-Optimal Reaction Wheel Attitude Control," *Journal of Guidance, Control, and Dynamics*, Vol. 35, No. 4, 2012, pp. 1208–1217.

[15] P. Tsiotras, H. Shen, and C. Hall, "Satellite Attitude Control and Power Tracking with Energy/Momentum Wheels," *Journal of Guidance, Control, and Dynamics*, Vol. 24, Jan. 2001, pp. 23–34, 10.2514/2.4705.

[16] D. A. Dueri, B. A. Acikmese, and F. A. Leve, "Reaction wheel dissipative power reduction control allocation via lexicographic optimization," *AIAA/AAS Astrodynamics Specialist Conference*, 2014, p. 4103.

[17] B. Wie, *Space Vehicle Dynamics and Control*. AIAA Education Series, AIAA, Reston, VA., Second ed., 2008.

[18] I. M. Ross and F. Fahroo, "Legendre Pseudospectral Approximations of Optimal Control Problems," *Kang, W. et al. (eds.) Lecture Notes in Control and Information Sciences*, Vol. 295, pp. 327–342, Springer, New York, 2003.

[19] I. M. Ross, *A Primer on Pontryagin's Principle in Optimal Control, second edition*. Collegiate Publishers, San Francisco, CA, 2015.

[20] I. M. Ross and M. Karpenko, "A Review of Pseudospectral Optimal Control: from Theory to Flight," *Annual Reviews in Control*, Vol. 36, No. 2, 2012, pp. 182–197.

[21] Q. Gong, W. Kang, and I. M. Ross, "A Pseudospectral Method for the Optimal Control of Constrained Feedback Linearizable Systems," *IEEE Transactions on Automatic Control*, Vol. 51, No. 7, 2006, pp. 1115–1129.

[22] W. Kang, Q. Gong, I. Ross, and F. Fahroo, "On the convergence of nonlinear optimal control using pseudospectral methods for feedback linearizable systems," *International Journal of Robust and Nonlinear Control*, Vol. 17, No. 14, 2007, pp. 1251–1277.

[23] I. M. Ross, R. J. Proulx, M. Karpenko, and Q. Gong, "Riemann-Stieltjes Optimal Control Problems for Uncertain Dynamical Systems," *Journal of Guidance, Control, and Dynamics*, Vol. 38, July 2015, pp. 1251–1263.

[24] I. M. Ross, "A Historical Introduction to the Convector Mapping Principle," *Proceedings of Astrodynamics Specialists Conference*, Monterey, CA, 2005.

[25] Q. Gong, I. M. Ross, W. Kang, and F. Fahroo, "Connections between the covector mapping theorem and convergence of pseudospectral methods for optimal control," *Computational Optimization and Applications*, Vol. 41, No. 3, 2008, pp. 307–335.

[26] Q. Gong, I. M. Ross, and F. Fahroo, "Costate computation by a Chebyshev pseudospectral method," *Journal of Guidance, Control, and Dynamics*, Vol. 33, No. 2, 2010, pp. 623–628.

[27] M. Karpenko and R. J. Proulx, "Experimental Implementation of Riemann–Stieltjes Optimal Control for Agile Imaging Satellites," *Journal of Guidance, Control, and Dynamics*, Vol. 39, No. 1, 2015, pp. 144–150.

[28] N. Bedrossian, S. Bhatt, M. Lammers, L. Nguyen, and Y. Zhang, "First Ever Flight Demonstration of Zero Propellant Maneuver Attitude Control Concept," *Guidance, Navigation, and Control Conference*, Hilton Head, South Carolina, 2007, pp. AIAA–2007–6734.

[29] N. S. Bedrossian, S. Bhatt, W. Kang, and I. M. Ross, "Zero-propellant Maneuver Guidance," *IEEE Control Systems Magzine*, Vol. 29, No. 5, 2009, pp. 53–73.

[30] W. Kang and N. Bedrossian, "Pseudospectral Optimal Control Theory Makes Debut Flight — Saves NASA $1M in Under 3 hrs," *SIAM news*, Vol. 40, No. 7, 2007.

[31] S. Bhatt, N. S. Bedrossian, Longacre, and L. Nguyen, "Optimal Propellant Maneuver Flight Demonstration on ISS," *AIAA Guidance, Navigation and Control Conference*, No. AIAA 2013-5027, Boston, MA, Aug 19-22 2013.

[32] M. Karpenko, S. Bhatt, N. Bedrossian, A. Fleming, and I. M. Ross, "First Flight Results on Time-Optimal Spacecraft Slews," *Journal of Guidance, Control, and Dynamics*, Vol. 35, No. 2, 2012, pp. 367–376.

[33] M. Karpenko, S. Bhatt, N. Bedrossian, and I. M. Ross, "Flight Implementation of Shortest-Time Maneuvers for Imaging Satellites," *Journal of Guidance, Control, and Dynamics*, 2014, pp. 1–11.

[34] N. Bedrossian, M. Karpenko, and S. Bhatt, "Overclock My Satellite," *IEEE Spectrum*, Vol. 49, No. 11, 2012, pp. 54–62.

[35] H. Schaub, *Analytical Mechanics of Space Systems*. AIAA Education Series, AIAA, Reston, VA, Third ed., 2003.

[36] F. L. Markley, "Attitude Estimation or Quaternion Estimation?," *Journal of Astronautical Sciences*, Vol. 52, No. 1, 2004, pp. 221–238.

[37] B. Bialke, "High fidelity mathematical modeling of reaction wheel performance," *Guidance and control 1998*, 1998, pp. 483–496.

[38] B. Wie and J. Lu, "Feedback Control Logic for Spacecraft Eigenaxis Rotations Under Slew Rate and Control Constraints," *Journal of Guidance, Control, and Dynamics*, Vol. 18, No. 6, 1995, pp. 1372–1379.

[39] F. Clarke, "Optimization and Nonsmooth Analysis (SIAM, New York, 1990)," *Reprint, originally published: Wiley, New York*, 1983.

[40] F. H. Clarke, Y. S. Ledyaev, R. J. Stern, and P. R. Wolenski, *Nonsmooth analysis and control theory*, Vol. 178. Springer Science & Business Media, 2008.

[41] I. M. Ross, "Space Trajectory Optimization and L1-Optimal Control Problems," *Modern astrodynamics*, Vol. 1, 2006, p. 155.

[42] W. Kang, Q. Gong, and I. M. Ross, "Convergence of pseudospectral methods for a class of discontinuous optimal control," *Proceedings of the 44th IEEE Conference on Decision and Control*, Seville, Spain, 2005, pp. 2799–2804.

[43] G. Q. K. M. Ross, I. M. and R. J. Proulx, "Scaling and Balancing for Faster Trajectory Optimization," *AAS/AIAA Astrodynamics Specialist Conference*, No. Paper number: AAS-17-675, Stevenson, WA, August 20 to August 24 2017.

[44] R. McHenry, A. Long, B. Cockrell, J. Thibodeau III, and T. Brand, "Space shuttle ascent guidance, navigation, and control," *Journal of the Astronautical Sciences*, Vol. 27, 1979, pp. 1–38.

[45] I. M. Ross, Q. Gong, F. Fahroo, and W. Kang, "Practical stabilization through real-time optimal control," *American Control Conference, 2006*, IEEE, 2006, pp. 6–pp.

[46] E. Ahronovich and M. Balling, "Reaction Wheel and Drive Electronics For LeoStar Class Space Vehicles," 1998.